NASA Technical Memorandum 87115
IAF-85-282

Surface Temperature Distribution Along a Thin Liquid Layer Due to Thermocapillary Convection

(NASA-TM-87115) SURFACE TEMPERATURE DISTRIBUTION ALONG A THIN LIQUID LAYER DUE TO THERMOCAPILLARY CONVECTION (NASA) 14 p HC A02/MF A01 CSCL 20D
N85-34357
Unclas
G3/34 22233

Chun-Liang Lai and An-Ti Chai
Lewis Research Center
Cleveland, Ohio

Prepared for the
XXXVIth International Astronautical Congress
sponsored by the International Astronautical Federation
Stockholm, Sweden, October 7-12, 1985

NASA

SURFACE TEMPERATURE DISTRIBUTION ALONG A THIN LIQUID LAYER

DUE TO THERMOCAPILLARY CONVECTION

Chun-Liang Lai* and An-Ti Chai
National Aeronautics and Space Administration
Lewis Research Center
Cleveland, Ohio 44135
U.S.A.

E-2715

SUMMARY

The surface temperature distributions due to thermocapillary convections in a thin liquid layer with heat fluxes imposed on the free surface are investigated. The nondimensional analysis predicts that, when convection is important, the characteristic length scale in the flow direction L, and the characteristic temperature difference ΔT_0, can be represented by $L \sim (A^2 Ma)^{1/4} L_R$ and $\Delta T_0 \sim (A^2 Ma)^{-1/4} \Delta T_R$, respectively, where L_R and ΔT_R are the reference scales used in the conduction-dominant situations with A denoting the aspect ratio and Ma the Marangoni number. Having had L and ΔT_0 defined, the global surface-temperature gradient $(\Delta T_0/L)$, the global thermocapillary driving-force, and other interesting features can then be readily determined. Finally, numerical calculations involving a Gaussian heat flux distribution are presented to justify these two relations.

INTRODUCTION

The availability of a low-gravity environment aboard a spacecraft opens new possibilities for the growth of better quality crystals. Among various techniques used for crystal growth, containerless processes such as the floating-zone method seem to have a very great potential to benefit from the space environment.

In the floating-zone method, a nonuniform heat flux imposed along the free surface of the melt may induce a thermocapillary flow in the melt if the surface is reasonably free from contamination. Chang and Wilcox (1975, 1976) investigated floating-zone problems numerically by assuming a vertical cylindrical melt with planar solid-liquid interfaces. Clark and Wilcox (1980) later pointed out and corrected certain errors in Chang and Wilcox's numerical formulation. The main feature of the numerical work is the prediction of flow cells (toroidal vortices) that extend through the entire fluid. Unfortunately, these numerical studies were limited to cases with small Marangoni numbers (1 to 10) which are too small to simulate actual situations, which are typically on the order of magnitude of greater than 10^2.

In order to simplify the analysis, most of the studies in the past dealt with the flow phenomena in a half-zone configuration (Chun, 1980a - Lai, 1984; Ostrach, Kamotani, and Lai, 1985; Preisser, Scharmann, and Schwabe, 1981 - Schwabe and coworkers, 1978; Vargas, Ostrach, and Kamotani, 1982). In these

---

*National Research Council - NASA Research Associate.

models a liquid bridge is suspended vertically between two circular rods with a higher temperature at the upper rod and a lower temperature at the bottom one. Several investigators have also studied the flow phenomena in a two-dimensional slot with different temperatures specified on the side walls (Lai, 1984; Sen and Davis, 1982; Strani, Piva and Graziani, 1983). The thermocapillary convections in a two-dimensional thin liquid layer with specified surface temperature distributions were also studied in the past (Lai, 1984; Pimputka and Ostrach, 1980; Smith and Davis, 1983a, 1983b). However, the coupling among the flow field, the temperature field and the imposed heat flux was not taken into consideration. In order to demonstrate certain features due to such a coupling, a simple model is being proposed in this investigation.

The proposed model is essentially a two-dimensional thin liquid layer with a nonuniform heat flux imposed on the free surface. It differs from those in the past studies in that convection is considered to be of primary importance in the present model. Consequently, the coupling effect mentioned above can no longer be ignored. Among several important and interesting features of the thermocapillary flows, the surface temperature distribution is one of the most critical factors because it determines the driving force of the thermocapillary flows. In contrast to the conduction-dominant situations, the surface temperature distribution due to thermocapillary convection in a thin liquid layer with a nonuniform heat flux imposed on the free surface is determined by the coupling among the flow field, the temperature field and the imposed heat flux. The surface temperature distribution itself is a part of the solution. Consequently, any estimation of the global surface-temperature gradient based on the information derived from the conduction-dominant situations will be inappropriate. Without the correct information about the global surface temperature distribution, a proper estimation of the driving force and, hence, other information about the thermocapillary flow cannot be obtained. Furthermore, for a two-dimensional thermocapillary convection experiment, if the dimension in the flow direction is not designed large enough, sharp surface temperature variations in the corner regions near the lower temperature side walls will exist. This sharp surface temperature variation will bring about strong shear stresses in corner regions, which, under certain circumstances, may induce unsteady flows. Lowry (1980) experimentally studied a similar problem using a two-dimensional container with a horizontal heating element located symmetrically above the free surface of the fluid sample. The velocity and temperature distributions were measured for several different cases, but the relationship between the surface temperature distribution and the coupling was not taken into consideration. As a result there has been no guidance for modeling or designing an experiment to avoid sharp surface-temperature variations which are known to exist in the corner regions near the lower temperature side walls. The present study is aimed at resolving all these deficiencies.

Dimensional analysis with proper balancing between physical quantities is employed initially to obtain appropriate dimensionless parameters. Based on these parameters, the characteristic temperature difference along the free surface ΔT_0 and the characteristic length scale in the flow direction L can be determined. Having had these two quantities defined, the global surface-temperature gradient $\Delta T_0/L$, the global driving force, and other interesting features such as the characteristic velocity can be realistically assessed. A numerical calculation is used to verify the validity of the parameters obtained in the first part of the present study. Hopefully, this effort will lead to a better understanding of certain important and interesting features of thermocapillary flows.

MATHEMATICAL FORMULATION AND DIMENSIONAL ANALYSIS

As a result of the coupling among the flow field, the temperature field, and the imposed heat flux, the surface temperature becomes a part of the solution itself when convection becomes important. The purpose of this section is to obtain a proper estimation of such a surface temperature distribution.

The schematic diagram of the configuration and the applied coordinate system of the present study are shown in figure 1. The problem considered herein is a steady, two-dimensional thermocapillary convection in a thin liquid layer (i.e., inertia effects are negligible) with nonuniform heat fluxes imposed on the free surface. For simplicity, but without losing the generality, a Gaussian-distributive heat flux is considered in the present study. The bottom boundary is kept at the lower ambient temperature. Under the thin layer configuration, buoyancy force is negligibly small compared to the thermocapillary driving-force. The dimensionless governing equations and boundary conditions are as follows:

$$\frac{\partial u}{\partial x} + \frac{\partial v}{\partial y} = 0 \tag{1}$$

$$\frac{\partial^2 u}{\partial y^2} = \frac{\partial p}{\partial y} \tag{2}$$

$$\frac{\partial p}{\partial y} = 0 \tag{3}$$

$$A^2 Ma\left(u \frac{\partial \theta}{\partial x} + v \frac{\partial \theta}{\partial y}\right) = \frac{\partial^2 \theta}{\partial y^2} \tag{4}$$

$$\frac{\partial u}{\partial y}(x,1) = -\frac{\partial \theta}{\partial x}(x,1) \quad \text{at the free surface} \tag{5}$$

$$\frac{\partial \theta}{\partial y}(x,1) = e^{-x^2} \quad \text{at the free surface} \tag{6}$$

$$u(x,0) = \theta(x,0) = 0 \quad \text{at the bottom wall} \tag{7}$$

$$\frac{\partial \theta}{\partial x}(0,y) = 0 \tag{8}$$

where (u,v) is the dimensionless velocity vector, p is the dimensionless pressure, θ is the dimensionless temperature difference, A is the aspect ratio, and Ma is the Marangoni number. In the above formulation, the free surface is assumed to be flat, and the heat loss from the free surface is neglected. In addition, the following nondimensionalization scheme has been employed:

$$x \sim L_R,\ y \sim D,\ u \sim \frac{D}{L_R}\,\frac{|\sigma_T|\Delta T_R}{\mu},\ v \sim \frac{D^2}{L_R^2}\,\frac{|\sigma_T|\Delta T_R}{\mu},\ p \sim \frac{|\sigma_T|\Delta T_R}{D},\ \theta \sim \Delta T_R$$

where μ denotes the dynamic viscosity, σ_T is the surface-tension gradient with respect to temperature T, D is the layer depth, L_R is the characteristic length scale of the imposed heat flux. Let f_0 be the amplitude of the Gaussian-distributive heat flux and k be the thermal conductivity. Then $\Delta T_R = f_0 D/k$ gives the referenced temperature difference. It is derived from the energy boundary condition at the free-surface by assuming conduction as dominant.

The dimensionless parameters involved are

aspect ratio $A = \frac{D}{L_R}$

Marangoni number $Ma = \frac{D|\sigma_T|\Delta T_R}{\mu\alpha}$

where α is the thermal diffusivity. When convection becomes important, that is, when $(A^2 Ma) \gg 1$, L_R and ΔT_R are no longer the proper characteristic quantities because they are derived under conduction dominant conditions. The global surface-temperature gradient based on the ratio of these two quantities, $\Delta T_R/L_R$, becomes therefore incorrect. To obtain appropriate estimations of a proper length scale L and a proper characteristic temperature difference ΔT_0 in terms of L_R, ΔT_R, and $A^2 Ma$, the following argument is made.

In the steady state, L and ΔT_0 can be properly determined from the global energy-balance condition (i.e., the energy input from the imposed heat flux should be equated to the energy output by conduction through the bottom wall) and the local energy boundary condition at the center point (0,1) of the free surface, where the temperature reaches its maximum value. The global energy-balance condition indicates that

$$f_0 L_R \sim k \frac{\Delta T_0}{D} L$$

or

$$\frac{L_R}{L} \sim \frac{\Delta T_0}{(f_0 D/k)} = \frac{\Delta T_0}{\Delta T_R} \qquad (9)$$

The expression $k(\Delta T_0/D)$ has been used above to estimate the global heat flux through the bottom wall. This implies that, in the steady state, convection should finally be balanced by conduction across the entire layer. Otherwise, convection will keep heating up the liquid in the downstream until the flow field eventually reaches the steady state. But at the central position, where the thermal boundary layer has not been developed to the full layer depth, the use of D as the characteristic length scale for the conduction in y-direction will be improper. The local energy boundary condition at the center point of the free surface (eq. (6)) indicates that

$$f_o \sim k \frac{\Delta T_o}{\delta_T}$$

where δ_T denotes the thermal boundary layer thickness at the central position, which is obtained by balancing conduction and convection in the y-direction at that position. Let

$$U_o^* = \frac{D}{L} \frac{|\sigma_T| \Delta T_o}{\mu} \quad \text{and} \quad V_o^* = \frac{D}{L} U_o^*$$

be the characteristic velocities in the x- and y- directions, respectively, when convection becomes important, and $A^* = D/L$ and $Ma^* = (U_o^* L/\alpha)$, the corresponding modified aspect ratio and Marangoni number; then, by the balance between convection and conduction in the y-direction at the central position,

$$\delta_T \sim \frac{D}{\left(DV_o^*/\alpha\right)} = \frac{D}{A^{*2} Ma^*}$$

Therefore,

$$f_o \sim k \frac{\Delta T_o}{(D/A^{*2} Ma^*)}$$

and (using eq. (9))

$$\frac{\Delta T_o}{(f_o D/k)} = \frac{\Delta T_o}{\Delta T_R} \sim \frac{L_R}{L} \sim \frac{1}{A^{*2} Ma^*} \tag{10}$$

Because

$$A^{*2} Ma^* = \frac{D^2}{L^2} \frac{U_o^* L}{\alpha} = \left(\frac{L_R}{L}\right)^3 (A^2 Ma)$$

and equation (10) applies,

$$\left(\frac{L_R}{L}\right)^3 (A^2 Ma) \sim \frac{L}{L_R}$$

and

$$\left(\frac{L}{L_R}\right)^4 \sim A^2 Ma$$

Now we have the following two relations:

$$L \sim (A^2 Ma)^{1/4} L_R \tag{11}$$

and

$$\Delta T_o \sim (A^2Ma)^{-1/4} \Delta T_R \tag{12}$$

Equations (11) and (12) indicate that L is directly proportional to $(A^2Ma)^{1/4}$ and ΔT_0 is inversely proportional to $(A^2Ma)^{1/4}$ when convection is important. These two relations also indicate that as convection becomes more and more dominant, that is, when the value of A^2Ma becomes larger, more heat gets transported downstream by thermocapillary convection. As a result of this, the characteristic temperature difference is reduced to a smaller portion of ΔT_R. These two relations are shown in figure 2 and will be verified in the next section when numerical calculations are presented.

A further remark should be made with regard to the values of $A^{*2}Ma^*$. Combining equation (10) with equation (11) or (12) yields

$$A^{*2}Ma^* \sim (A^2Ma)^{1/4}$$

This implies that, in the steady-state, although the convection should finally be balanced by the conduction in a thin liquid layer as discussed earlier, it is inadequate to require $A^{*2}Ma^* \sim 1$. The unusual result is due to the deceleration of the surface velocity in thermocapillary flows (i.e., from U_0^* to zero at a far downstream point of the flow field), which allows the thermal boundary layer to grow faster than expected.

NUMERICAL CALCULATIONS

In the thin liquid layer analysis, as the velocity field is coupled with the temperature field only through the shear-stress boundary condition at the free surface (eq. (5)), the momentum equation (eq. (2)) can be solved first. The solutions of u(x,y) and v(x,y) are

$$u(x,y) = -\frac{d\theta_s}{dx}\left(\frac{3}{4}y^2 - \frac{1}{2}y\right)$$

and

$$v(x,y) = \frac{1}{4}\frac{d^2\theta_s}{dx^2}(y^3 - y^2)$$

where $\theta_s(x)$ is the dimensionless surface-temperature distribution. The expressions of u and v also satisfy the continuity equation. The energy equation (eq. (4)) becomes, after substituting the above expressions for u and v,

$$A^2Ma\left[-\frac{d\theta_s}{dx}\left(\frac{3}{4}y^2 - \frac{1}{2}y\right)\frac{\partial\theta}{\partial x} + \frac{1}{4}\frac{d^2\theta_s}{dx^2}(y^3 - y^2)\frac{\partial\theta}{\partial y}\right] = \frac{\partial^2\theta}{\partial y^2}$$

Because of the local nonlinearity (i.e., the existence of $[(d\theta_s/dx)(\partial\theta/\partial x)]$ and $[(d^2\theta_s/dx^2)(\partial\theta/\partial y)]$ in the convection terms), it is still very difficult to obtain the analytical solution of $\theta(x,y)$. In this section, a finite difference numerical scheme is employed to calculate the temperature distributions $\theta(x,y)$ for different values of A^2Ma.

Instead of solving the steady state equation, a time dependent term is included for the time marching procedure. The equation to be solved becomes

$$\frac{\partial\theta}{\partial t} + A^2Ma\left[-\frac{d\theta_s}{dx}\left(\frac{3}{4}y^2 - \frac{1}{2}y\right)\frac{\partial\theta}{\partial x} + \frac{1}{4}\frac{d^2\theta_s}{dx^2}(y^3 - y^2)\frac{\partial\theta}{\partial y}\right] = \frac{\partial^2\theta}{\partial y^2}$$

The main features of the numerical scheme employed in the present study can be outlined as follows:

(1) Central differences are used for both the first and second derivatives except at the boundaries where suitable boundary conditions are incorporated.

(2) Because of the modest variations, the grid spacing for the numerical calculation are chosen to be 0.1 in both xand y-directions.

(3) Depending on the magnitude of A^2Ma, proper time intervals are chosen for the time marching procedures so that stable numerical calculations can be obtained.

(4) To determine the steady-state, a proper criterion ϵ is used for the temperature difference calculated at two time steps. The criterion depends on the magnitude of A^2Ma and the global energy balance between the imposed heat flux and the heat conduction through the bottom wall (to be within $\sim10^{-2}$ difference). As an example, the criterion ϵ used for the case with $A^2Ma = 10^4$ is $\sim10^{-3}$ for two calculations at one-thousand time steps apart.

(5) In order to reduce the computation time, the domain of calculation is increased successively when appropriate. That is, when the temperature at the last grid point reaches 0.002, another ten more grid points at the downstream are then added to the calculation domain until the temperature field finally reaches the steady-state. The initial domain used for calculation is 30 grid spaces in the x-direction (i.e., up to $x = 3$) and 10 grid spaces in the y-direction (i.e., up to $y = 1$, the free surface).

Since the detailed temperature distributions of the whole flow field are not of interest to the present study, only the surface temperature distributions for various situations are recorded and plotted in order to verify the theoretical predictions made in the previous section. The surface temperature distributions for various values of A^2Ma are shown in figure 3. It can be seen that as the convection become more important, that is, as the value of A^2Ma increases, the extent of the surface temperature distribution becomes larger. Consequently, the dimensionless temperature difference at the central position decreases, that is, the characteristic temperature difference ΔT_0 becomes a smaller portion of the referenced temperature difference ΔT_R. These two behaviors had been predicted by nondimensional analysis discussed in the previous section. The relations of the characteristic length scale L and the characteristic temperature difference ΔT_0 versus A^2Ma are shown in logarithmic scales in figure 2. Although the numerical calculations of the characteristic temperature difference do not appear to coincide with the theoretical line, they are within the same order of magnitude. In the non-dimensional analysis with order-of-magnitude estimates, the power law is of primary concern. It can be seen from figure 2 that both the theoretical predictions and the numerical calculations follow the same trends. This confirms the validity of equations (11) and (12).

SUMMARY AND CONCLUSIONS

The thermocapillary convection in a liquid phase with a nonuniform heat flux imposed on the free surface is a very practical and important problem related to the floating-zone crystal growth. For simplicity, a two-dimensional thin liquid layer is employed herein to investigate the effect on surface temperature distribution due to the coupling among the flow field, the temperature field and the imposed heat flux. The following conclusions are drawn from the analysis made in the present study:

1. Dimensional analysis and the numerical calculations indicate that for thermocapillary convection flow in a thin layer configuration, the following two relations are valid:

$$L \sim (A^2 Ma)^{1/4} L_R$$

and

$$\Delta T_o \sim (A^2 Ma)^{-1/4} \Delta T_R$$

With L and ΔT_o determined, the global surface-temperature gradient, the thermocapillary driving force and other important information such as the characteristic velocity can be assessed properly.

2. With the above two relations, proper experimental designs for the investigation of the thermocapillary convections can be made to avoid the sharp surface-temperature variations in the corner regions near side walls. Effects due to strong shear stresses in corner regions near the side walls can then be reasonably eliminated in such a configuration and if an unsteady, oscillatory motion is found, it can be attributed to coupling among the flow field, the temperature field and the imposed heat flux.

REFERENCES

Chang, C.E. and Wilcox, W.R. (1975). Inhomogeneities Due to Thermocapillary Flow in Floating Zone Melting. J. Cryst. Growth, 28, 8-12.

Chang, C.E. and Wilcox, W.R. (1976). Analysis of Surface Tension Driven Flow in Floating Zone Melting. Int. J. Heat Mass Transfer, 19, 355-366.

Chun, Ch.-H (1980a). Marangoni Convection in a Floating Zone Under Reduced Gravity. J. Cryst. Growth, 48, 600-610.

Chun, Ch.-H (1980b). Experiments on Steady and Oscillatory Temperature Distribution in a Floating Zone Due to the Marangoni Convection. Acta Astronaut., 7, 479-488.

Chun, Ch.-H and Wuest, W. (1978). A Micro-Gravity Simulation of the Marangoni Convection. Acta Astronaut., 5, 681-686.

Chun, Ch.-H and Wuest, W. (1979). Experiments on the Transition from the Steady to the Oscillatory Marangoni-Convection of a Floating Zone Under Reduced Gravity Effect. Acta Astronaut., 6, 1073-1082.

Clark, P.A. and Wilcox, W.R. (1980). Influence of Gravity on Thermocapillary Convection in Floating Zone Melting of Silicon. J. Cryst. Growth, 50, 461-469.

Fu, B.-I. and Ostrach, S. (1983). Numerical Solutions of Thermocapillary Flows in Floating Zones. In, M.M. Chen, J. Mazumder, C.L. Tucker (Eds.), Transport Phenomena in Materials Processing, ASME, New York, pp. 1-10.

Kamotani, Y., Ostrach, S. and Vargas, M. (1984). Oscillatory Thermocapillary Convection in a Simulated Floating-Zone Configuration. J. Cryst. Growth, 66, 83-90.

Lai, C.L. (1984). Studies of Thermocapillary Oscillation Phenomena. Ph. D. Dissertation, Department of Mechanical and Aerospace Engineering, Case Western Reserve University.

Lowry, S. (1980). An Experimental Study of Heat Induced Surface Tension Driven Flow. M. S. Thesis, Department of Mechanical and Aerospace Engineering, Case Western Reserve University.

Ostrach, S., Kamotani, Y. and Lai, C.L. (1985). Oscillatory Thermocapillary Flows. PCH Physicochemical Hydrodynamics, (to be published).

Pimputkar, S.M. and Ostrach, S. (1980). Transient Thermocapillary Flow in Thin Liquid Layers. Phys. Fluids, 23, 1281-1285.

Preisser, F., Scharmann, A. and Schwabe, D. (1981). Oscillatory Motion of Thermocapillary Convection in Floating Zones. In, European Mechanics Colloquium, 138, Univ. Karlsruhe.

Schwabe, D. (1981). Marangoni Effects in Crystal Growth Melts. PCH, Physicochem. Hydrodyn., 2, 263-280.

Schwabe, D. and Scharmann, A. (1979). Some Evidence for the Existence ad Magnitude of a Critical Marangoni Number for the Onset of Oscillatory Flow in Crystal Growth Melts. J. Cryst. Growth, 46, 125-131.

Schwabe, D., Scharmann, A. and Preisser, F. (1981). Verification of the Oscillatory State of Thermocapillary Convection in a Floating Zone Under Low Gravity. Acta Astronaut., 9, 265-273.

Schwabe, D., Scharmann, A., Preisser, F. and Oeder, R. (1978). Experiments on Surface Tension Driven Flow in Floating Zone Melting. J. Cryst. Growth, 43, 305-312.

Sen, A.K. and Davis, S.H. (1982). Steady Thermocapillary Flows in Two-Dimensional Slots. J. Fluid Mech., 121, 163-186.

Smith, M.K. and Davis, S.H. (1983a). Instabilities of Dynamic Thermocapillary Liquid Layers, Part 1: Convective Instabilities. J. Fluid Mech., 132, 119-144.

Smith, M.K. and Davis, S.H. (1983b). Instabilities of Dynamic Thermocapillary Liquid Layers, Part 2: Surface-Wave Instabilities. J. Fluid Mech., 132, 145-162.

Strani, M., Piva, R. and Graziani, G. (1983). Thermocapillary Convection in a Rectangular Cavity: Asymptotic Theory and Numerical Simulation. J. Fluid Mech., 130, 347-376.

Vargas, M., Ostrach, S. and Kamotani, Y. (1982). Surface Tension Driven Convection in a Simulated Floating Zone Configuration. M.S. Thesis, Department of Mechanical and Aerospace Engineering, Case Western Reserve University (also FTAS/TR-82-159).

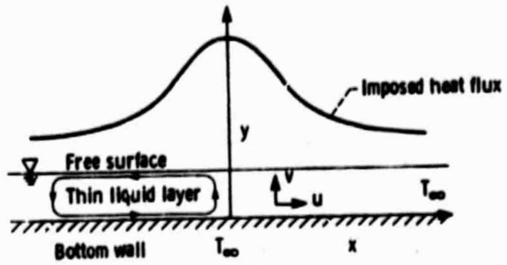

Fig. 1. Geometrical configuration and the coordinate system.

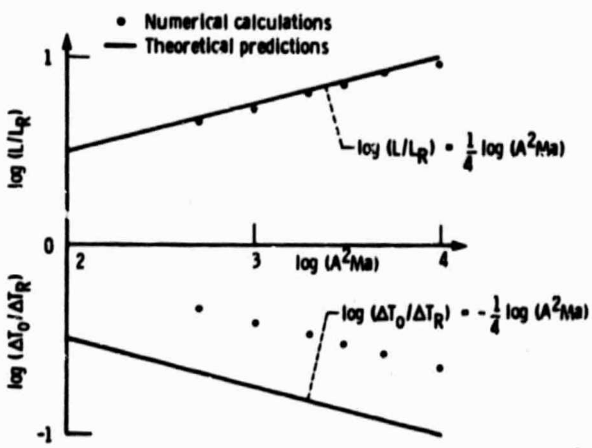

Fig. 2. Relations of $\log(L/L_R)$ and $\log(\Delta T_0/\Delta T_R)$ versus $\log(A^2 Ma)$.

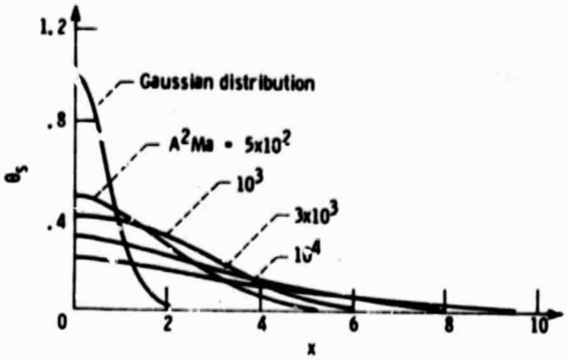

Fig. 3. Surface temperature distributions for various values of (A^2Ma).

1. Report No. NASA TM-87115 IAF-85-282	2. Government Accession No.	3. Recipient's Catalog No.

4. Title and Subtitle	5. Report Date
Surface Temperature Distribution Along a Thin Liquid Layer Due to Thermocapillary Convection	6. Performing Organization Code 674-25-05
7. Author(s) Chun-Liang Lai and An-Ti Chai	8. Performing Organization Report No. E-2715
	10. Work Unit No.
9. Performing Organization Name and Address National Aeronautics and Space Administration Lewis Research Center Cleveland, Ohio 44135	11. Contract or Grant No.
	13. Type of Report and Period Covered Technical Memorandum
12. Sponsoring Agency Name and Address National Aeronautics and Space Administration Washington, D.C. 20546	14. Sponsoring Agency Code

15. Supplementary Notes
Chun-Liang Lai; National Research Council - NASA Research Associate; An-Ti Chai, NASA Lewis Research Center. Report prepared for the XXXVIth International Astronautical Congress, sponsored by the International Astronautical Federation, Stockholm, Sweden, October 7-12, 1985.

16. Abstract
The surface temperature distributions due to thermocapillary convections in a thin liquid layer with heat fluxes imposed on the free surface are investigated. The nondimensional analysis predicts that, when convection is important, the characteristic length scale in the flow direction L, and the characteristic temperature difference ΔT_0 can be represented by $L \sim (A^2 Ma)^{1/4} L_R$ and $\Delta T_0 \sim (A^2 Ma)^{-1/4} \Delta T_R$, respectively, where L_R and ΔT_R are the reference scales used in the conduction-dominant situations with A denoting the aspect ratio and Ma the Marangoni number. Having had L and ΔT_0 defined, the global surface-temperature gradient ($\Delta T_0/L$), the global thermocapillary driving-force, and other interesting features can then be readily determined. Finally, numerical calculations involving a Gaussian heat flux distribution are presented to justify these two relations.

17. Key Words (Suggested by Author(s))	18. Distribution Statement
Thermocapillary convection; Thin liquid layer; Marangoni number; Free surface; Floating-zone; Coupling	Unclassified - unlimited STAR Category 34

19. Security Classif. (of this report)	20. Security Classif. (of this page)	21. No. of pages	22. Price*
Unclassified	Unclassified		

*For sale by the National Technical Information Service, Springfield, Virginia 22161